PLOS PATHOGENS

RESEARCH ARTICLE

Zinc-finger (ZiF) fold secreted effectors form a functionally diverse family across lineages of the blast fungus *Magnaporthe oryzae*

Juan Carlos De la Concepcion[1,2¤a]*, Thorsten Langner[2¤b], Koki Fujisaki[3], Xia Yan[2], Vincent Were[2], Anson Ho Ching Lam[1¤c], Indira Saado[1], Helen J. Brabham[2], Joe Win[2], Kentaro Yoshida[4], Nicholas J. Talbot[2], Ryohei Terauchi[3,5], Sophien Kamoun[2], Mark J. Banfield[1]*

1 Department of Biochemistry and Metabolism, John Innes Centre, Norwich Research Park, Norwich, United Kingdom, **2** The Sainsbury Laboratory, University of East Anglia, Norwich Research Park, Norwich, United Kingdom, **3** Division of Genomics and Breeding, Iwate Biotechnology Research Center, Iwate, Japan, **4** Laboratory of Plant Genetics, Graduate School of Agriculture, Kyoto University, Kyoto, Japan, **5** Laboratory of Crop Evolution, Graduate School of Agriculture, Kyoto University, Kyoto, Japan

¤a Current address: Gregor Mendel Institute of Molecular Plant Biology, Austrian Academy of Sciences, Vienna, Austria
¤b Current address: Department of Molecular Biology, Max Planck Institute for Developmental Biology, Tubingen, Germany
¤c Current address: Department of Cell and Developmental Biology, John Innes Centre, Norwich Research Park, Norwich, United Kingdom
* juan.concepcion@gmi.oeaw.ac.at; mark.banfield@jic.ac.uk

Citation: De la Concepcion JC, Langner T, Fujisaki K, Yan X, Were V, Lam AHC, et al. (2024) Zinc-finger (ZiF) fold secreted effectors form a functionally diverse family across lineages of the blast fungus *Magnaporthe oryzae*. PLoS Pathog 20(6): e1012277. https://doi.org/10.1371/journal.ppat.1012277

Editor: Richard A. Wilson, University of Nebraska-Lincoln, UNITED STATES

Received: October 23, 2023

Accepted: May 20, 2024

Published: June 17, 2024

Data Availability Statement: The authors confirm that all data underlying the findings are fully available without restriction. All relevant data are within the paper and its Supporting Information files.

Funding: This work was supported by the Biotechnology and Biological Sciences Research Council (BBSRC, UK, grants BB/WW002221/1 and BB/V002937/1 to SK; BB/V016342 to NJT; BB/V015508/1 to MJB; BB/P012574 to MJB, SK and

Abstract

Filamentous plant pathogens deliver effector proteins into host cells to suppress host defence responses and manipulate metabolic processes to support colonization. Understanding the evolution and molecular function of these effectors provides knowledge about pathogenesis and can suggest novel strategies to reduce damage caused by pathogens. However, effector proteins are highly variable, share weak sequence similarity and, although they can be grouped according to their structure, only a few structurally conserved effector families have been functionally characterized to date. Here, we demonstrate that Zinc-finger fold (ZiF) secreted proteins form a functionally diverse effector family in the blast fungus *Magnaporthe oryzae*. This family relies on the Zinc-finger motif for protein stability and is ubiquitously present in blast fungus lineages infecting 13 different host species, forming different effector tribes. Homologs of the canonical ZiF effector, AVR-Pii, from rice infecting isolates are present in multiple *M. oryzae* lineages. Wheat infecting strains of the fungus also possess an AVR-Pii like allele that binds host Exo70 proteins and activates the immune receptor Pii. Furthermore, ZiF tribes may vary in the proteins they bind to, indicating functional diversification and an intricate effector/host interactome. Altogether, we uncovered a new effector family with a common protein fold that has functionally diversified in lineages of *M. oryzae*. This work expands our understanding of the diversity of *M. oryzae* effectors, the molecular basis of plant pathogenesis and may ultimately facilitate the development of new sources for pathogen resistance.

NJT; BBS/E/J/000PR9795 to MJB, SK and NJT; BBS/E/J/000PR9796 to MJB, SK and NJT; and BB/X010996/1 to MJB, SK and NJT). This work was also supported by The European Research Council (743165, "BLASTOFF" to SK and MJB); by The John Innes Foundation to JCDIC and AL; by The Gatsby Charitable Foundation to SK and NJT; and by The Japanese Society for the Promotion of Science (JSPS, KAKENHI 20H05681 to RT).The funders had no role in study design, data collection and analysis, decision to publish, or preparation of the manuscript.

Competing interests: SK receives funding from Industry on NLR biology.

Author summary

Diseases caused by filamentous plant pathogens impact global food production, leading to severe economic and humanitarian consequences. These pathogens secrete hundreds of effectors inside the host to alter cellular processes and to promote infection and disease. Effector proteins have weak or no sequence similarity but can be grouped in structural families based on conserved protein folds. However, very few conserved effector families have been functionally characterized. We have identified a family of effectors with a shared Zinc-finger protein fold (ZiF) that is present in lineages of the blast fungus *Magnaporthe oryzae* that can, collectively, infect 13 different grasses. We characterized the binding of a sub-set of these proteins to putative Exo70 host targets and showed they can be recognized by the plant immune system. Furthermore, we show that other ZiF effectors do not bind Exo70 targets, suggesting functional specialization within this effector family for alternative interactors. These findings shed light on the diversity of effectors and their molecular functions, as well as potentially leading to the development of new sources of blast disease resistance.

Introduction

Pathogens have evolved sophisticated strategies to overcome host defences and manipulate cellular pathways to promote their proliferation. One such strategy is to deploy effector proteins into the host. These effectors carry out multiple functions within the host cell, including plant immune suppression and metabolic manipulation [1]. In general, effectors can be very diverse, sharing low or no sequence similarity. Despite their intrinsic variability, effectors can share similar protein folds and be grouped into structurally related families [2–6]. Elucidation of experimental structures of fungal effectors and advances in computational structure prediction have revealed how these proteins, which typically have low amino acid sequence conservation, can share similar protein folds [3,7–13]. However, although effector proteins can be classified according to their predicted structure, only a few structurally conserved effector families have been functionally characterized to date.

Blast disease, caused by the ascomycete fungus *Magnaporthe oryzae*, affects a wide variety of grasses including staple food crops such as rice, barley, and wheat in addition to many other grass species causing significant losses in food production required to feed the world's population [14–16]. The blast fungus is thought to be undergoing incipient speciation into genetically distinct lineages that are typically associated with a single grass host genus [17,18]. *M. oryzae* infects multiple wild grasses that often occur in close proximity to crops, acting as a pathogen reservoir [19] that, together with the potential for host jumps and reassortment of the effector repertoire [20,21], makes this pathogen a significant threat to food security even in areas where blast disease is not endemic [19]. Therefore, understanding the virulence mechanisms and effector biology of *M. oryzae* is important to achieve resistance and develop new strategies to mitigate its economic impact [22,23].

The genome of *M. oryzae* encodes hundreds of putative effectors [24]. For example, the rice blast strain Guy11 has at least 546 effector proteins [25]. To date, most structurally characterized blast fungus effectors share the same protein fold. Structural studies of the effectors AVR--Pik, AVR1-CO39, AVR-Pia, AVR-Pizt and AVR-Pib revealed they all share a six-strand β-sandwich fold, comprised of two antiparallel β-sheets [7,26–28]. This was designated as the

MAX (for Magnaporthe Avrs and ToxB like) effector fold and was used to define a diverse and expanded effector family in blast genomes comprising 5 to 10% of all putative effectors [7].

Studies focused on the biology of MAX effectors have demonstrated how these effectors target host proteins [21,29,30], how they are detected by the plant immune system [26,27,31–33], and how this interaction has shaped the evolution of host immunity [34,35]. These studies have led to the first steps in the development of synthetic intracellular immune receptors with bespoke pathogen recognition [36–41], a goal long pursued in plant biotechnology [22,23,42]. Despite this progress, studies addressing functional characterization and experimental determination of non-MAX effectors from *M. oryzae* have remained somewhat behind in comparison to MAX effectors.

Recently, we determined the structure of the non-MAX effector AVR-Pii in complex with its host target [43]. AVR-Pii is a secreted small effector protein that binds to two Exo70 proteins, OsExo70F2 and OsExo70F3, both putative components of the rice exocyst complex [43,44]. The physical interaction between AVR-Pii and these Exo70 proteins is recognized by the rice Pii NLR pair (Pii-1 and Pii-2), triggering immune responses that halt colonization by *M. oryzae* [44,45]. Even though their molecular cloning was reported at the same time [46,47], AVR-Pii remained understudied compared with the MAX effectors AVR-Pik and AVR-Pia. AVR-Pii is absent in most rice blast isolates and was not found in preliminary effector searches in isolates infecting other cereals [48,49].

The structure of AVR-Pii bound to OsExo70F2 identified a new effector/target molecular interface with the potential to suggest the virulence-associated mechanism of this effector and inform the development of bespoke resistance by engineering effector recognition in NLRs [43]. Interestingly, the structure also revealed a novel effector fold comprising a Zinc-finger domain, coined the Zinc-finger effector fold (ZiF), which is distinct in sequence and structure from the MAX fold previously identified for *Magnaporthe* effectors [43]. Understanding the diversity and structure / function relationships of ZiF effectors could help guide bioengineering of novel disease resistance genes.

Here, we tested the importance of residues forming the Zinc-finger in AVR-Pii function and folding, as a general model for ZiF effectors. We used the structural information of the AVR-Pii fold to guide a Hidden Markov Model search into the genomes of *M. oryzae* infecting diverse grasses to identify effectors sharing the ZiF fold. We report and categorize the presence of a family of ZiF effector proteins prevalent across blast lineages and show that different ZiF effector tribes likely target different host proteins, implying functional diversity. We show that, just like rice blast AVR-Pii, some wheat blast ZiF effectors bind host Exo70s and can be recognized by Pii resistance, establishing a potential novel approach for developing disease resistance against the emerging wheat blast pathogen.

Results

The Zinc-finger motif of AVR-Pii is required for protein stability and binding to host Exo70 proteins

The recently determined structure of AVR-Pii revealed a new fold for a *M. oryzae* effector based on a Zinc-finger formed by residues Cys51, Cys54, His67 and Cys69 [43]. Although not directly involved in the effector/target binding interface, random mutagenesis assays suggest that mutating these residues has a negative effect on interaction with the host target OsExo70F3 [43]. To better understand the role of the AVR-Pii Zinc-finger motif, we mutated residues Cys51, Cys54 and His67 to Alanine (AVR-Pii^{CCH}) and tested for interaction with rice Exo70 targets, OsExo70F2 and OsExo70F3, by Yeast-2-Hybrid (Y2H) and *in planta* co-immunoprecipitation (Co-IP) (**Fig 1**).

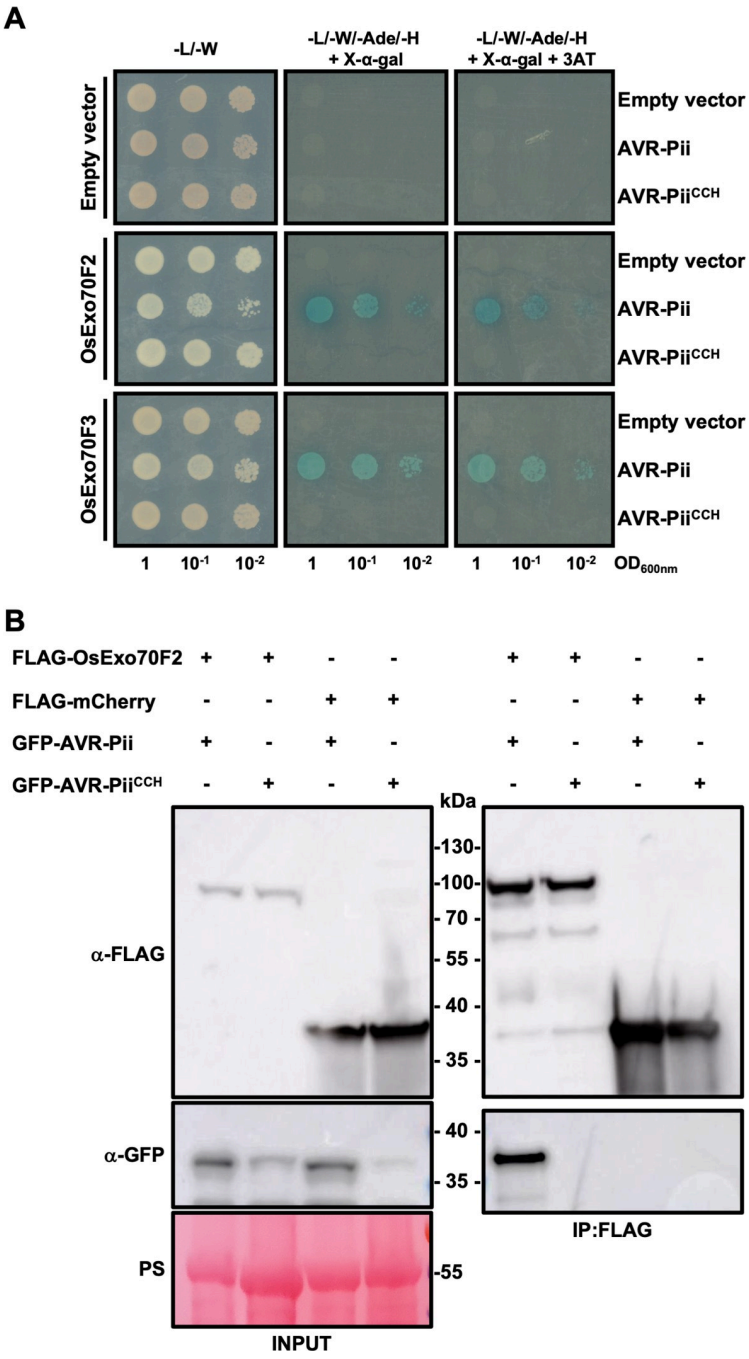

Fig 1. Mutations in AVR-Pii Zinc-finger motif abrogate binding to Exo70 host target. (A) Yeast two-hybrid assay of AVR-Pii and AVR-Pii^{CCH} with OsExo70F2 or OsExo70F3 host targets. For each combination, 5μl of yeast were spotted and incubated in double dropout plate for yeast growth control (left) and quadruple dropout media supplemented with X-α-gal and 3AT (right). Growth, and development of blue coloration, in the selection plate are both indicative of protein:protein interaction. OsExo70 proteins were fused to the GAL4 DNA binding domain and AVR-Pii to the GAL4 activator domain. Empty vectors were used as negative control in each combination. **(B)** Co-immunoprecipitation of AVR-Pii and AVR-Pii^{CCH} with OsExo70F2. N-terminally GFP-tagged AVR-Pii effectors were transiently co-expressed with N-terminally 3xFLAG-tagged OsExo70F2 or 3xFLAG-mCherry in *N. benthamiana*. Immunoprecipitates (IPs) were obtained with anti-FLAG magnetic beads and total protein extracts were probed with appropriate antisera.

https://doi.org/10.1371/journal.ppat.1012277.g001

As previously reported, co-expression of wild-type AVR-Pii with rice OsExo70F2 or OsExo70F3 supports yeast growth on selective media and development of blue coloration as readouts of protein-protein interactions (**Fig 1A**) [43,44]. By contrast, co-expression with AVR-Pii^{CCH} did not induce growth or development of blue coloration, indicating that these mutations affect effector binding to the host target (**Fig 1A**). Further, accumulation of the AVR-Pii^{CCH} protein was consistently lower in yeast cells, when compared with the wild-type effector, which may account for some of the differences observed (**S1 Fig**). We tested whether mutations in the Zinc-finger motif of AVR-Pii also alters protein accumulation in plant cells. For this, we transiently expressed an N-terminally SH-tagged version of AVR-Pii^{CCH} in *Nicotiana benthamiana* and a 3xFLAG-tagged version in rice protoplasts. Compared to wild-type AVR-Pii, the stability of the Zinc-finger mutant was also compromised in plant cells (**S2 Fig**), further supporting the role of this motif in maintaining an appropriate protein fold.

To discern whether disruption of the AVR-Pii Zinc-finger motif affects binding to OsExo70 targets beyond reduced effector accumulation, we tested the association of GFP-AVR-Pii^{CCH} to 3xFLAG-OsExo70F2 by Co-IP (**Fig 1B**). While AVR-Pii successfully associated with OsExo70F2, AVR-Pii^{CCH} was not able to associate (**Fig 1B**), confirming the results obtained in the Y2H assay (**Fig 1A**).

Together, we confirmed the importance of the Zinc-finger motif for AVR-Pii function, showing that mutations in the zinc-binding motif compromise protein stability and abrogate binding to effector targets, most likely due to disruption of the protein fold.

An HMM-based search of *M. oryzae* proteomes reveals a family of Zinc-finger (ZiF) fold effectors with similarity to AVR-Pii

Genome-wide searches for putative effectors, and their grouping into families, is facilitated by structural information [7,8,12,50,51]. Given the importance of AVR-Pii residues in forming the ZiF fold, and consequently for function and stability, we reasoned they would be a conserved core maintained during evolution and could be a signature to search and identify related blast effectors.

To test this hypothesis, we generated a hidden Markov model (HMM) representing the ZiF fold from *M. oryzae* sequences closely related (BLASTP E-value $\leq 1 \times 10^{-4}$) to AVR-Pii and performed an HMM search against existing proteomes of *M. oryzae* [48,52]. The HMM search reported 227 hits with scores ranging from 10.3 to 58.0. We removed 111 redundant sequences that showed 100% sequence identity to query sequences and 83 without effector characteristics, such as the presence of a secretion peptide, resulting in 33 ZiF effectors from the searched proteomes (Fig 2A and S1 Data).

ZiF effectors are widespread in host-specialized genetic lineages of the blast fungus

To identify the prevalence and diversity of ZiF effectors across all available genome assemblies of *Magnaporthe spp*., we performed TBLASTN searches for each of 33 ZiF effectors across 107 *M. oryzae* genome assemblies infecting 13 grass species as reported previously [21]. We manually inspected the output and collected new variants of ZiF effectors that showed similarity to queries with E-value less than or equal to 1×10^{-10}, have no premature stop codon, have no deletion/insertion in their sequences, and still maintain ZiF fold residues. In total, we obtained 95 non-redundant ZiF effectors from publicly available proteomes and genomes of *Magnaporthe spp*.

We classified this set of 95 ZiF effectors using TRIBE-MCL approach into 10 different tribes ranging in size from 68 to 119 residues (**Figs 2A and S3A and S2 Data**). AVR-Pii belongs to

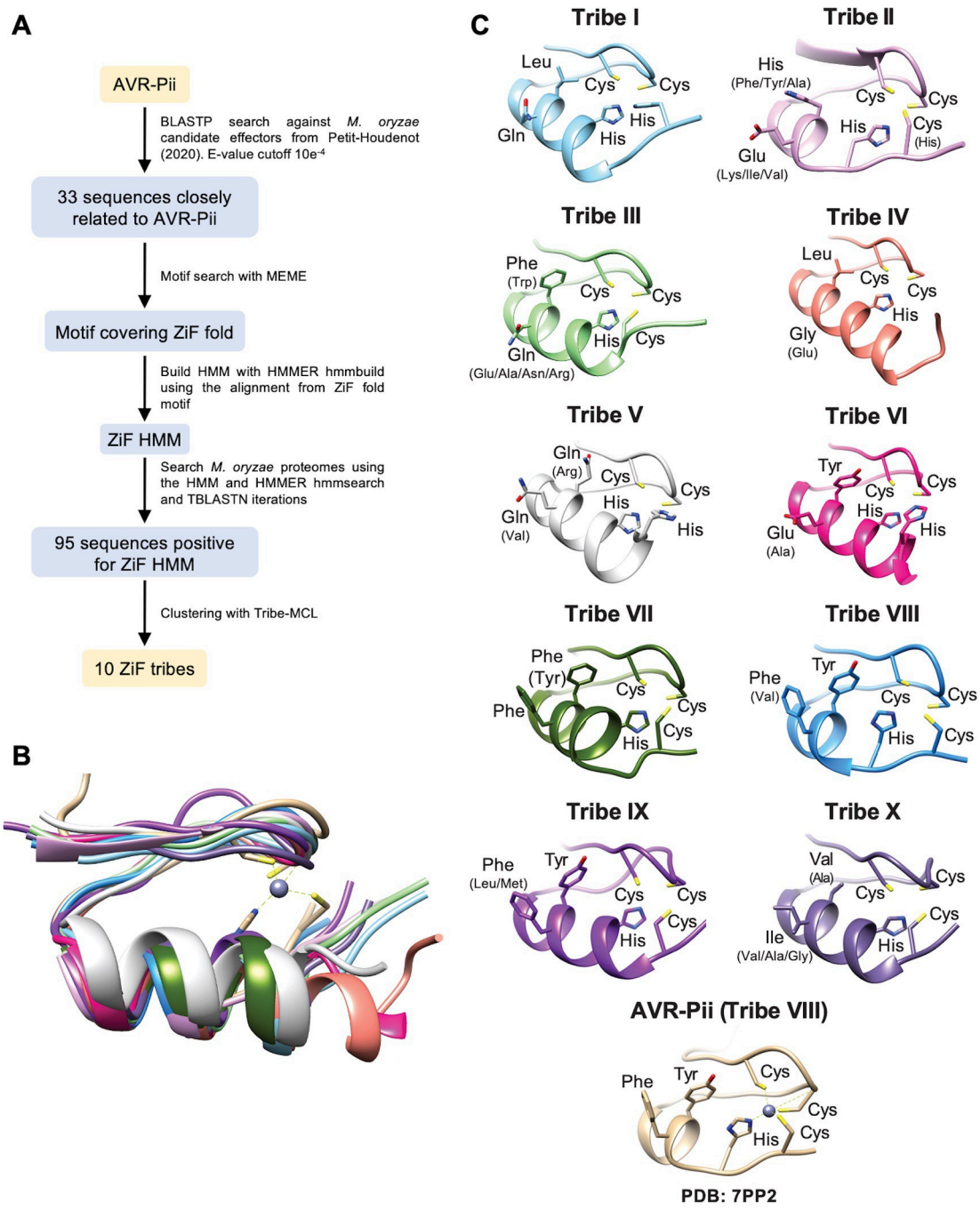

Fig 2. AVR-Pii Zinc-finger Fold (ZiF) defines an effector family in *M. oryzae*. **(A)** Workflow of HMM-based search for Zinc-finger fold effectors. Schematic representation of the ZiF motif search pipeline and results. **(B)** Superimposition of the ZIF fold of AVR-Pii (light brown) and representative members of all ZIF effector tribes of *M. oryzae*. **(C)** Alphafold2 models of amino acid residues that form the binding interface and the zinc finger motif. Amino acid variation within tribes is shown in parentheses. The experimental model of AVR-Pii (PDB: 7PP2) is added as a reference.

https://doi.org/10.1371/journal.ppat.1012277.g002

tribe VIII, which contains 7 different alleles (S3A Fig). While the sequence similarity between ZiF effector tribes is highly divergent (S3A Fig), structure prediction by Alphafold2 identified the presence of a ZiF fold in all the tribes (Fig 2B and 2C).

To find out whether the ZiF HMM model could detect all 95 ZiF effectors, we ran hmmsearch using the ZiF HMM identified above. We found that 93 showed hits with scores ranging from 6.1 to 58.0 (**S3B Fig**). Two ZiF effectors with no hit were IIa and Va. Similarly, we used the Avr-Pii amino acid sequence in a BLASTP search against the ZiF effector tribes. We found that 91 Zif effectors had hits to Avr-Pii with BLASTP score ranging from 15.8 to 147 (or E-value from 4.4 to 2 x 10^{-51}). Four did not have a hit to Avr-Pii (**S3B Fig**).

Next, we noted the presence/absence of each ZiF effector tribe to every genome of the genetic lineage of *M*. *oryzae* (**Fig 3**). For each isolate, we report the absence of a ZiF tribe when TBLASTN did not find a significant hit, and the presence on detection of one or more hits. We also investigated the genomic position of these hits, to consider whether a blast isolate harbours more than one member of a particular ZiF effector tribe. We further define cases of pseudogenized ZiF effectors when the hit from TBLASTN misses a start codon, are truncated, carry an early stop codon, and/or are missing the predicted Zinc-finger motif.

Despite AVR-Pii being reported as absent in most rice infecting blast isolates, our analysis found that most of the ZiF effector family tribes are present in all *M*. *oryzae* genomes examined (**Fig 3**). Several of the ZiF effector tribes are also present in the genomes of the more distantly related *Magnaporthe grisea* isolates infecting crabgrass (*Digitaria sanguinalis*) and fountain grass (*Pennisetum americanum*) (**Fig 3**). The allelic distribution and sequences of ZiF effectors in each blast lineage can be found in (**S3 Data and S4 Data**).

Interestingly, some ZiF effector tribes showed lineage-specific patterns of presence/absence polymorphism (**Fig 3**), which could be associated with colonization of a different host (host jump) [20], or to the genetic conflict with an immune receptor recognizing the effector [49]. For example, most rice-infecting *M*. *oryzae* isolates lack members from the ZiF tribe VIII, which includes AVR-Pii, likely because of the deployment of the Pii resistance in rice (**Fig 3**). Furthermore, rice blast isolates did not harbour any member of tribe IX, which may indicate the presence of selective pressure to the pseudogenization of members of this tribe from rice-infecting blast isolates. We also find similar patterns in non-rice infecting *M*. *oryzae* isolates, such as those infecting foxtail millet (*Setaria spp*.), ryegrass (*Lolium spp*.), signalgrass (*Brachiaria spp*.) and Goosegrass (*Eleusine spp*.) where some specific tribes have been deleted or pseudogenized (**Fig 3**). Together, this data shows that ZiF effectors form a conserved family in *Magnaporthe* genomes and illustrate the presence of lineage-specific selective pressure that generates specific patterns of effector presence/absence, likely through the genetic conflict with plant immune receptors from different plant species.

ZiF effectors have different expression patterns during infection

Magnaporthe effectors are commonly upregulated during infection [7,12,25,53]. To look for ZiF effector expression during infection, we screened a time-resolved transcriptome of Guy11 infecting the rice cultivar CO39 [25] (**S4 Fig and S5 Data**).

Blast strain Guy11 only contains ZiF effectors from the tribe I, III, IV, V, VI, VII and X (it does not harbour a functional copy of AVR-Pii) (**Fig 3**) and we could only detect expression for tribes I, VI and X, meaning that ZiF effector tribes III, IV, V and VII are not expressed (or are under the detectable range) during Guy11 infection on CO39 rice cultivars.

ZiF effectors from tribe I and X have their maximum expression peak at 24 and 48 hours after infection (hpi), suggesting a role of these effectors during biotrophic colonization (**S4 Fig and S5 Data**). By contrast, the effector from ZiF tribe VI is expressed at 96 hpi, which may indicate a role during later stages of the infection (**S4 Fig and S5 Data**).

Both tribe I and X have two paralogs in the genome of Guy11 and they have differences in their expression patterns, suggesting some possible non-overlapping roles of effectors from the

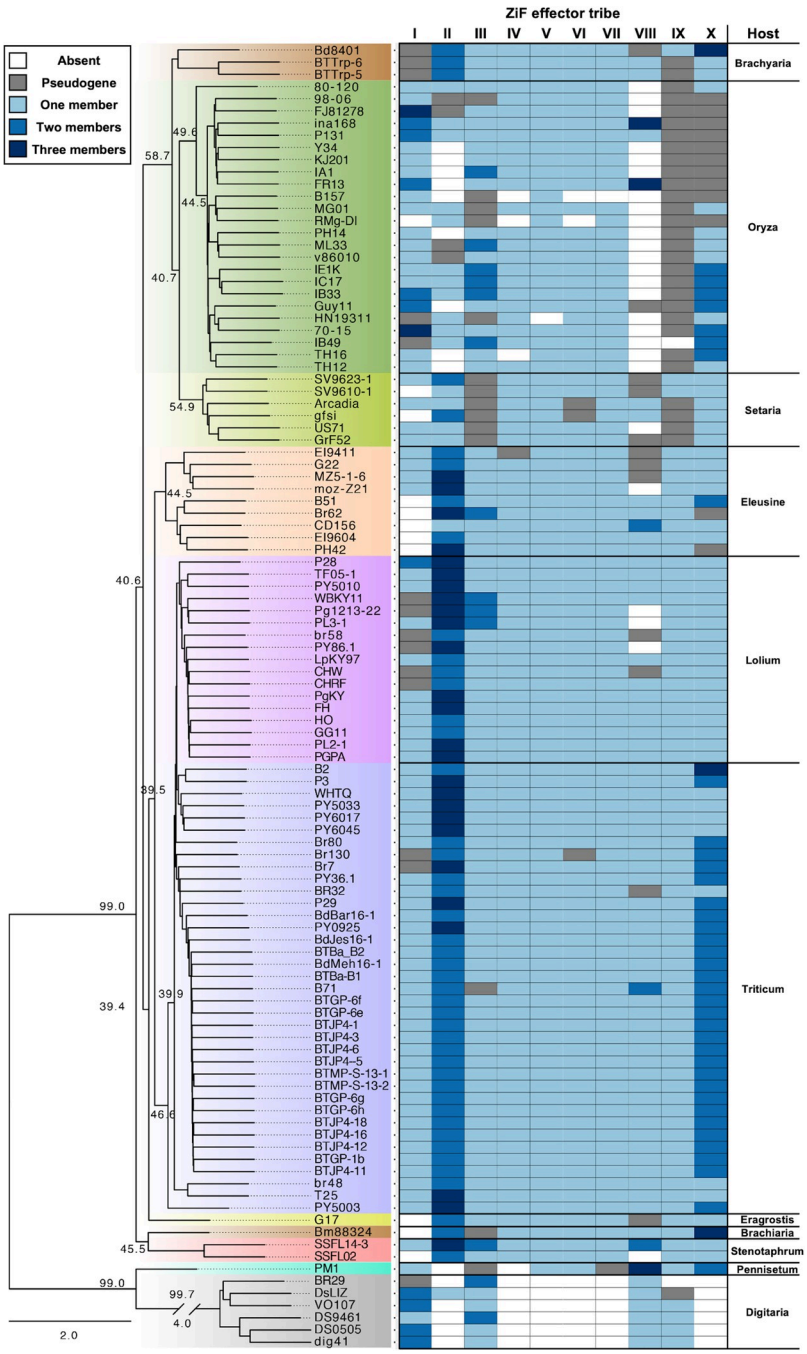

Fig 3. Zif effectors are conserved across different host-specific lineages of *M. oryzae*. Presence/absence analysis of ZiF effector tribes across host-specific lineages of *M. oryzae*. An ASTRAL multispecies coalescence tree (reprinted of a figure panel from Bentham et al. [21]) is shown on the left. On the right, we indicate the presence of ZiF effectors for each tribe in every blast isolate. ZiF tribes without presence in the genome of a blast isolate is represented as white. The presence of a pseudogenized effector (no start codon and/or truncation of the ZiF fold) are represented in grey. When more than one member of the same ZiF effector tribe is present, it is represented in different shades of blue.

https://doi.org/10.1371/journal.ppat.1012277.g003

same tribe. Both ZiF_If and ZiF_Ik have their expression height at 24 hpi, however, ZiF_Ik could be detected at 16hpi but not at 48 hpi while ZiF_If is clearly expressed at 48 hpi but not before 24 hpi (**S4 Fig and S5 Data**). In the case of tribe X this difference is more extreme as we

find expression of ZiF_Xp at 24 and 48 hpi but we detect no expression of the other member of the tribe, ZiF_Xi (**S4 Fig and S5 Data**).

When considered together, these observations provide evidence that ZiF effectors are differentially expressed during pathogen colonization, and therefore likely to carry out diverse roles during infection.

An AVR-Pii-like ZiF effector from wheat blast lineages binds Exo70s

Despite being absent in most rice-infecting *M. oryzae* isolates, AVR-Pii-like tribe VIII is highly conserved in wheat blast lineages, including the pandemic B71 clonal lineage [16], and the host Exo70 binding residues identified for AVR-Pii (VIIId) [43] are conserved in the wheat blast counterpart (VIIIc) (**S5 Fig**).

We used Y2H to compare the binding of these two effectors to the Exo70 target. This assay showed that both effectors interact with OsExo70F3, inducing a nearly similar growth of yeast in selective media and development of blue coloration (**Fig 4A**). To test whether the binding interface previously described for AVR-Pii [43] is functionally conserved in the wheat blast counterpart, we introduced a Phe66Glu mutation in ZiF_VIIIc. This mutation essentially prevented binding to the host target OsExo70F3 in a yeast-2-hybrid assay (**Fig 4A**), confirming that this effector uses the same surface to bind Exo70 as AVR-Pii (ZiF_VIIId) [43]. Both effectors accumulated at similar levels in yeast cells (**S6 Fig**).

As ZiF effectors from Tribe VIII are conserved in non-rice infecting isolates, we investigated the presence of potential host Exo70 targets in grasses other than rice. For this, we analysed the conservation of the effector binding interface in recently annotated Exo70F2 and Exo70F3 proteins from eight grass species including rice, wheat, barley and foxtail millet [54]. This sequence alignment showed that, with the exception of Exo70F2 in Foxtail millet, there is conservation of the hydrophobic pocket where ZiF effectors could likely bind via the docking of a Phe residue, as identified in the AVR-Pii/Exo70F2 complex [43] (**S7 Fig**).

Our data reveal that effectors belonging to the conserved ZiF tribe VIII in *M. oryzae* isolates infecting wheat and other grasses can potentially bind to host Exo70 proteins from clade F in a similar manner as described for the rice blast effector AVR-Pii.

Zif effectors conserved in wheat blast lineages can be recognized by the rice NLR Pii

ZiF effectors from tribe VIII are conserved in wheat infecting lineages of *M. oryzae*, notably the pandemic clone B71 that is threatening wheat production in three continents [16] harbours at least two copies (**Fig 3**). Given that ZiF_VIIIc, an effector from Tribe VIII of wheat-infecting isolates, interacts with Exo70 host proteins in a similar way to AVR-Pii (**Fig 4**), we tested whether this effector triggers Pii-mediated resistance.

For this, we cloned ZiF_VIIIc from the wheat-infecting *M. oryzae* isolate BTJP 4–1 and transformed into the rice-infecting isolate Sasa2, which lacks AVR-Pii, and tested pathogen recognition by rice cultivar Moukoto (Pii-) and Hitomebore (Pii+) (**Figs 4B and S8**). Spot inoculation assays showed that Sasa2 transformants harbouring the BTJP 4–1 ZiF_VIIIc effector become avirulent on Hitomebore but not on Moukoto (**Figs 4B and S8**). This recognition is consistent with the result of Sasa2 transformants harbouring AVR-Pii (**Figs 4B and S8**) [43,44,46]. We also included in the assay wheat-infecting M. oryzae isolates Br32 and BTJP 4–1 although, as expected, they were unable to infect either Moukoto or Hitomebore plants (**Figs 4B and S8**). Additionally, we performed spray inoculation assays and obtained results consistent with those from spot inoculation (**Figs 4C and S9**).

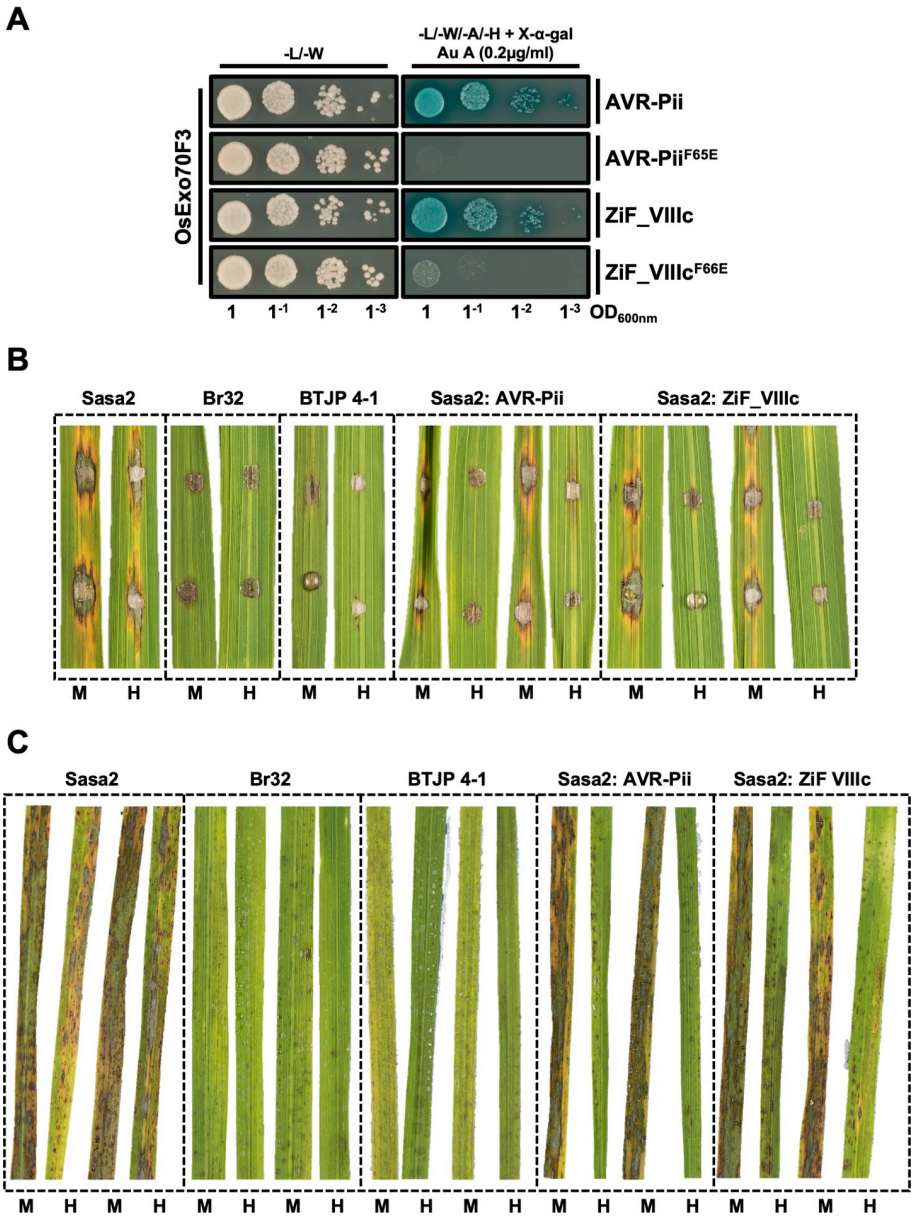

Fig 4. Wheat blast AVR-Pii homolog ZiF_VIIIc binds to OsExo70F3 and is recognized by Pii resistance in rice. **(A)** Y2H assay of wild-type AVR-Pii and ZiF_VIIIc and their corresponding mutants at the host target binding interface (Phe65Glu and Phe66Glu, respectively) to host target OsExo70F3. Left, control plate for yeast growth. Right, quadruple-dropout media supplemented with X-α-gal and aureobasidine A (Au A). Growth and development of blue coloration in the right panel indicates protein-protein interactions. OsExo70F3 was fused to the GAL4 DNA binding domain while effectors were fused to the GAL4 activator domain. Each experiment was repeated a minimum of three times, with similar results. **(B)** Rice leaf blade spot inoculation of transgenic *M*. *oryzae* Sasa2 isolates expressing AVR-Pii or ZiF_VIIIc from wheat blast isolate BTJP 4–1 in rice cultivars Moukoto (Pii-) and Hitomebore (Pii+). The cultivars Moukoto and Hitomebore are denoted by M and H, respectively. For each experiment, a representative image from replicates with independent *M*. *oryzae* transformants are shown. Wild-type rice blast isolate Sasa2 and wheat blast Br32 and BTJP 4–1 are included as control. Full images for the three experimental replicates are presented in S8 Fig. **(C)** Spray inoculation of transgenic *M*. *oryzae* isolates in 3-weeks-old rice cultivar Moukoto and Hitomebore. Each experiment was performed four times (two of the leaves are shown for the Sasa2, Br32 and BTJP 4–1 isolates). All leaf images are shown in S9 Fig.

https://doi.org/10.1371/journal.ppat.1012277.g004

Together, our data shows that conserved ZiF effectors present in wheat-infecting *M. oryzae* isolates can be recognized by Pii-mediated resistance in rice. This presents new opportunities to explore the transfer of Pii-mediated resistance from rice into other grasses affected by blast disease, including wheat and barley.

Diverse tribes of ZiF effectors may have different host targets

Although ZiF effectors from different tribes are predicted to share structural similarity (**Fig 2**), the residues of AVR-Pii that mediate binding to OsExo70 targets are not fully conserved between tribes (**S3 Fig**). We therefore hypothesised that some ZiF effector tribes might target other host proteins.

To test this, we selected the ZiF effector allele from each tribe that is most predominant in the genome of rice-infecting *M. oryzae* lineages (defined as the most common allele found in these genomes) and performed a Y2H assay to test for binding to OsExo70F3. ZiF_VIIId (AVR-Pii, the most representative allele of tribe VIII in rice isolates) and AVR-Pii Phe65Glu acted as positive and negative controls, respectively [43]. Interestingly, only ZiF_VIIc and ZiF_VIIId interacted with OsExo70F3 in this assay (**Fig 5A**). All ZiF effectors except ZiF_Xi were produced in yeast cells at similar levels to AVR-Pii (ZiF_VIIId) (**S10 Fig**). Our results showed that ZiF effectors from tribes other than VII and VIII do not interact with OsExo70F3 and may therefore have alternative host targets. The identification and characterisation of alternative host targets will be the subject of future work.

As host-specific *M. oryzae* effector alleles can differ in their association to host interactors [21], we extended the Y2H interaction assay with OsExo70F3 to ZiF effector alleles predominant in *M. oryzae* isolates infecting wheat, which have more representatives of ZiF tribes than rice-infecting isolates (**Fig 3**). Y2H assays showed that three of these tribes (VII, VIII and IX) interacted with OsExo70F3 (**Fig 5B**). All wheat blast ZiF effectors, except for ZiF_IVa and ZiF_Xi, had similar protein accumulation in yeast cells (**S11 Fig**).

Together, these Y2H assays indicate functional diversity in the host binding properties of ZiF effector family members, despite their conserved fold.

Discussion

The study of pathogen effectors and their functions has the potential to generate new biological understanding [47] and aid the development of disease management strategies to limit yield losses caused by biotic stress [22,23]. However, the high variability and diversity of effectors at their sequence level, along with their typical small size, makes their classification and functional annotation from sequence challenging [5,55].

In this study, we showed how the ZiF protein fold observed in AVR-Pii [43] is essential for effector stability, and binding to host targets. We used this fold to define a diverse family of ~100 secreted proteins, uncovering a previously hidden conservation of these ZiF effectors across *M. oryzae* lineages infecting different grasses and opening new research avenues, both for discovering new effector activities and bioengineering disease resistance.

Previous classification of pathogen effectors into structurally related families based on HMM analysed required pre-existing experimental knowledge of the protein structure [7–9,51]. The revolution of protein fold prediction, largely fuelled by the release of AlphaFold2 [56], allowed the structural classification of effectors [3,4,50] and prediction of their targets [57] without the need of previous structural knowledge. Interestingly, structure prediction approaches did not identify the ZiF effector family in *M. oryzae* [3,4,50], showing how this approach can have limitations when it comes to small, unstructured protein sequences as often is the case of pathogen effectors.

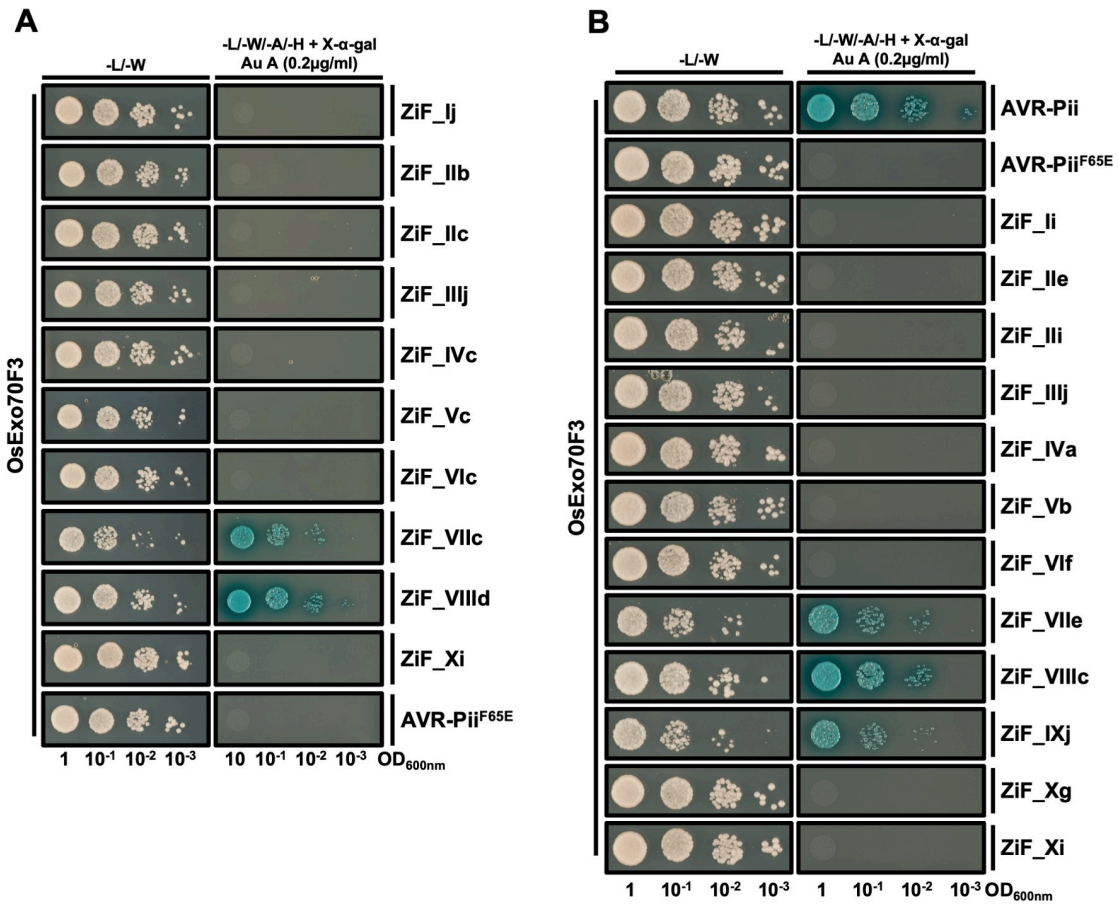

Fig 5. ZiF effectors do not share the same host target. (A) Y2H binding assay of ZiF effectors from rice blast isolates to host target OsExo70F3. For each tribe, the most prevalent allele in rice blast lineages was fused to the GAL4 activator domain and co-expressed in yeast cells with OsExo70F3 fused to GAL4 DNA binding domain. AVR-Pii Phe65Glu was used as negative control as previously reported [43]. **(B)** Y2H binding assay of ZiF effectors of wheat blast isolates to host target OsExo70F3. The most prevalent effector allele in each ZiF tribe of *M. oryzae* isolates infecting wheat was fused to the GAL4 activator domain and co-expressed in yeast cells with OsExo70F3 fused to GAL4 DNA binding domain. Rice blast AVR-Pii and AVR-Pii Phe65Glu were used as positive and negative controls, respectively. For both assays, a control plate for yeast growth is presented on the left and a plate with quadruple-dropout media supplemented with X-α-gal and aureobasidine A (Au A) is presented on the right. Growth and development of blue coloration in the right panel indicates protein-protein interactions. Each experiment was repeated a minimum of three times, with similar results.

https://doi.org/10.1371/journal.ppat.1012277.g005

For example, the fold of ~8000 from over 26000 secreted proteins could not be successfully predicted by AlphaFold2 in a large structural modelling study of secreted proteins from phytopathogenic fungi, including *M. oryzae* [3]. Moreover, over 30% of *M. oryzae* secreted proteins could not be predicted by TrRosetta [50] or AlphaFold2 [3]. With less than 100 residues and a large unstructured region at the N-terminus [43], AVR-Pii and other ZiF effectors are likely below the cutoff of structural prediction approaches. However, using the previously existing structure of AVR-Pii [43] could still successfully guide HMM searches to identify the ZiF family, illustrating how experimental knowledge of effector structures is still an important foundation for discoveries on effector biology [58].

Despite AVR-Pii being absent in most rice-infecting *M. oryzae* lineages [46,48,49], our combined MEME/HMM/TBLASTN approach uncovered a conservation of the ZiF effector family across all *M. oryzae* isolates. Some of the 10 ZiF tribes identified in this study display presence/absence patterns in some *M. oryzae* lineages, particularly those infecting rice.

Interestingly, wheat-infecting isolates conserve all ZiF effector tribes, possibly due to the recent expansion of these lineages [16] causing them to be less polymorphic in comparison to rice-infecting isolates.

An interesting case is the ZiF tribe VIII (that includes AVR-Pii), mostly absent in rice infecting isolates likely because of the deployment of the Pii resistance in rice. In contrast, all wheat-infecting isolates analysed here include a member of this effector tribe. This includes the pandemic B71 clonal lineage that has spread and caused disease in three continents [16]. We showed how ZiF_VIIIc from these lineages binds and triggers Pii resistance, suggesting the possibility of transferring Pii resistance from rice to wheat to deploy resistance against pandemic wheat blast strains.

We further identify two other ZiF effector tribes (VII and IX) that bind to OsExo70F3. Intriguingly, tribe VII effectors were found to not be expressed during rice infection experiments with isolate Guy11 (**S4 Fig**), and tribe IX members are pseudogenes in the genomes of rice-infecting isolates (**Fig 3**). Future work could test whether silencing or deletion of these effectors from the genome arose in these isolates to evade activation of Pii or any other resistance genes in rice. A recent study tested this hypothesis for *M*. *oryzae* MAX fold effectors that are deleted in the genomes of rice blast isolates, however, the authors could not validate that these effectors induce non-host resistance in rice [12].

Other putative effectors following presence/absence distributions are strong candidates for being recognised by a cognate resistance gene. For example, ZiF tribe II, which is absent in multiple rice-infecting lineages is duplicated in wheat-infecting *M*. *oryzae*, suggesting a resistance gene is present in rice that is unlikely to be *Pii* as the ZiF tribe II effector tested did not interact with OsExo70F3. Similarly, the absence of ZiF tribes in *M*. *oryzae* isolates infecting wild grasses, such as ZiF tribe I in *Brachyaria*- and *Eleusine*-infecting isolates, highlights the potential of finding new sources of resistance that could be deployed in cultivated grasses. Further, grass genomes encode NLR proteins with integrated Exo70 domains [59,60]. By increasing our knowledge of effectors that bind host Exo70 proteins, we have the potential to engineer Exo70 domains integrated in NLRs to bind and trigger immune responses against these effectors. A similar strategy has been successfully used for MAX effectors binding to HMA integrated domains [36–41].

Although ZiF effector tribes share the same fold, this is not necessarily predictive of protein function but may be involved in maintaining protein integrity while supporting sequence and functional diversification [7,21]. ZiF effectors have expanded in *M*. *oryzae* lineages and distribute in 10 tribes compared to *M*. *grisea* lineages, which presents only five. This expansion likely reflects a diversification in effector function. Two lines of evidence support of this possibility: First, a previous study reported that the ZiF effector ZiF_IVc (named MoHTR2) is nuclear localized and binds DNA for host transcriptional reprogramming [61], a function markedly different from the potential Exo70-binding related function of AVR-Pii. Second, we found that most ZiF effector tribes did not interact with the AVR-Pii host target, OsExo70F3, suggesting alternative targets. Future interaction screens are required to investigate the extent of targets bound by ZiF effectors, potentially generating new fundamental knowledge on *M*. *oryzae* virulence mechanisms, and helping guide classical breeding of disease resistance against rice and wheat blast.

Conclusion

In conclusion, we uncovered a family of effectors with structural similarity to the well-known *M*. *oryzae* effector AVR-Pii. This family clusters in 10 tribes with a shared fold based on a Zinc-finger motif. Although AVR-Pii is mostly absent in rice-infecting *M*. *oryzae* lineages, ZiF

effector tribes are prevalent in most *M*. *oryzae* lineages that infect different hosts. We showed that not all ZiF effector tribes share the same target and that AVR-Pii homologues from other lineages can be detected by Pii-mediated resistance from rice. This establishes the principle for investigating whether resistance deployed in rice could be transferred to other grasses as a strategy for developing resistance against pandemic fungal diseases such as wheat blast.

Materials and methods

Cloning of AVR-Pii for expression in planta

For the expression of GFP-tagged AVR-Pii or AVR-Pii^{CCH} in plant cells, we used the expression vector pICH47742 (https://synbio.tsl.ac.uk/). To generate a pICH47742-*MASPro*::GFP-AVR--Pii-MAS*Term* or pICH47742-*MASPro*::GFP-AVR-Pii^{CCH}-MAS*Term*, AVR-Pii and AVR--Pii^{CCH} cDNA was synthesized as PCR products (Gblocks, GeneWiz) with *Bsa*I restriction sites. All modules were assembled using the Golden Gate cloning. Restriction enzymes were purchased from New England Biolabs (Ipswich, MA, USA). Transient expression of GFP-AVR-Pii and GFP-AVR-Pii^{CCH} in *N*. *benthamiana* was performed as described below.

For the expression of StrepII-HA (SH) tagged AVR-Pii in plant cells, we used the expression vector pCAMBIA-SH-AVR-Pii previously described [44]. To generate a pCAMBIA--SH-AVR-Pii^{CCH} vector, AVR-Pii^{CCH} cDNA was artificially synthesized by GenScript Japan Inc (Tokyo, Japan) and the coding sequence was amplified by PCR using the primer set: KF1f (`5′-AATCACTAGTGGTGGCGGTCTTCCCACTCCGGCCAGCCTG-3′`) and KF118r (`5′-AATCCTGCAGTTAGTTGCATTTAGCATTAAAATA-3′`). Resulting PCR product was introduced into pCAMBIA-SH [44] using *Spe*I and *Pst*I sites. Transient expression of SH-AVR-Pii and SH-AVR-Pii^{CCH} mutant in *N*. *benthamiana* was performed as described previously [62].

For transient expression of 3xFLAG tagged AVR-Pii and AVR-Pii^{CCH} in rice protoplasts, we used the expression vectors pAHC-FL-AVR-Pii [44] and pAHC-AVR-Pii^{CCH}. For the construction of pAHC-FL-AVR-Pii^{CCH}, AVR-Pii^{CCH} cDNA was amplified by PCR using primer set; KF1f and KF3r (`5′- AATCGGATCCTTAGTTGCATTTAGCATTAAAATA -3′`). The resulting PCR product was exchanged with wild type AVR-Pii coding sequence of pAHC--FL-AVR-Pii using *Spe*I and *BamH*I sites.

Cloning of ZiF for Yeast-2-Hybrid assays

Coding sequences for the effector domain of the ZiF proteins reported here were synthesised as double-stranded DNA fragments (gBlocks, Integrated DNA Technologies). The fragments were subsequently inserted via BsaI in a pGADT7 vector adapted for Golden Gate cloning provided by the SynBio service at The Sainsbury Laboratory, Norwich.

To generate AVR-Pii^{CCH} mutant in pGADT7, AVR-Pii^{CCH} coding sequence was introduced into pGADT7 using EcoRI and BamHI sites following amplification by PCR using the following primer set: KF777f (`5′- CACCGAATTCCTTCCCACTCCGGCCAGC -3′`) KF780r (`5′- AACTGGATCCTTAGTTGCATTTAGCATTAAAAT -3′`)

Rice blast AVR-Pii and AVR-Pii Phe65Glu in pGADT7, as well as, OsExo70F3 in pGBKT7 were reported previously [43].

Cloning of ZiF_VIIIc from BTJP 4–1

DNA was extracted from *M*. *oryzae* isolate BTJP 4–1 using a CTAB method from mycelia grown on PDA plates. The effector AVR-Pii from was obtained via PCR amplification using Phusion Polymerase (New England Biolabs). Primers were designed on the promoter and terminator of ZiF_VIIIc from BTJP 4–1 and included the overhangs required for plasmid

assembly. Primer sequences used were: PCB1532_AVR-Pii_promoter_p1f (5'-AAGCTG-GAGCTCCACCGCGGCGCAGCAGAGGTCTAGTTTGAGCAC-3')

AVR-Pii_terminator_PCB1532_p1r (5'-CTATAGGGCGAATTGGGTACCTCGCATC GGCAAATACTCTCGAG-3')

The amplified fragment including promoter, CDS, and terminator was assembled into the backbone PCB1532 via In-Fusion cloning (In-Fusion cloning kit, Clontech Laboratories).

Transient expression in rice protoplasts

Rice protoplasts were isolated from rice cell culture [63,64]. For cell wall digestion, 5 ml of packed cell volume of cultured cells was mixed with 25 ml of cellulase solution [4% Cellulase RS (w/v; Yakult, Tokyo, Japan), 4% Cellulase R10 (w/v; Yakult), 0.1% $CaCl_2.6H_2O$ (w/v), 0.4M mannitol, 0.1% MES (w/v) pH5.6] and incubated with gentle shaking (60 rpm) at 30˚C for 3 h. After filtration through miracloth (Millipore, Billerica, MA), protoplasts in the flow through fraction were collected by centrifugation at 800 g and washed two times with 20 ml of W5 buffer (154 mM NaCl, 125 mM $CaCl_2$, 5mM KCl and 2mM MES pH5.7). Protoplast concentration was adjusted to 2–3 x 10^6 protoplasts/ml with W5 buffer. For transfection, 10 μg of plasmids pAHC-FL-AVR-Pii or pAHC-FL-AVR-Pii^{CCH} in a volume of 10 μl was mixed with 100 μl of protoplast solution. Next, 110 μl of PEG solution [40% PEG4000 (w/v; Fluka), 0.2M mannitol, 0.1M $CaCl_2$] was added to the protoplast solution, mixed gently, and incubated at room temperature for 20 min. Then, 700 μl of W5 buffer were added, and protoplasts were collected by centrifugation at 800 g. The protoplasts were washed with 700 μl of W5 buffer, resuspended with 500 μl of W5 buffer, and incubated in the dark at 30˚C for 20 h. After incubation, protoplasts were collected by 800 g centrifugation, resuspended with 60 μl of GSB buffer [62.5 mM Tris-HCl (pH6.8), 10% Glycerol, 0.2 g/ml SDS, 5μg/ml Bromophenol blue, and 100 mM DTT], and subjected to western blot assay using HRP-conjugated anti-FLAG M2 (Sigma-Aldrich, St. Louis, MO).

Protein-protein interaction: Yeast-2-hybrid assay

To test the interaction between AVR-Pii^{CCH} and OsExo70F3, Yeast-2-hybrid assays were performed as described previously [62]. Co-transformed yeast cells were prepared in a dilution series with OD_{600} = 3.0 (x1), 0.3 (x10^{-1}) and 0.03 (x10^{-2})] and spotted onto quadruple dropout medium (QDO); basal medium lacking Trp, Leu, Ade and His but containing 5-Bromo-4-Chloro-3- indolyl a-D-galactopyranoside (X-α-gal) (Clontech). To detect interactions, both QDO medium with and without 10 mM 3-amino-1,2,4-triazole (3AT) (Sigma) was used. Yeast cells were also spotted onto double dropout medium (DDO); basal medium lacking Trp, Leu to test cell viability.

To detect protein accumulation in yeast cells, cells were propagated in liquid DDO at 30˚C overnight. 40 mg of yeast cells were collected and resuspended with 160 ul GTN + DC buffer [10% glycerol, 25mM Tris-HCl (pH 7.5), 150mM NaCl, 1 mM DTT and 1 tablet of cOmplete EDTA-free (Roche, Basel Switzerland)]. Then, 160 μl of 0.6 N NaOH was added, mixed gently, and incubated at room temperature for 10 min. Next, 160 μl of gel sample buffer [40%(w/v) glycerol, 240 mM Tris-HCl pH 6.8, 8% (w/v) SDS, 0.04% (w/v) bromophenol blue, 400 mM DTT] was added and incubated at 95˚C for 5 min. After centrifugation at 20,000 g for 5 min, the supernatant was subjected to SDS-PAGE. Proteins expressed from bait and prey vectors were detected by using anti-Myc-tag mAb-HRP-DirectT (MBL, Nagoya, Japan) and anti-HA-Peroxidase 3F10 (Roche), respectively.

Yeast-2-hybrid assays of the interaction between ZiF effectors and the host target OsExo70F3 were performed as described previously [26,37,43]. In brief, pGADT7 plasmids

encoding the effector domain of different ZiF were co-transformed into chemically competent Y2HGold cells (Takara Bio, USA) with a pGBKT7 plasmid encoding OsExo70F3 in using a Frozen-EZ Yeast Transformation Kit (Zymo research).

After growing in selection plates, single co-transformants were inoculated in liquid SD-Leu-Trp media overnight at 30˚C. The saturated culture was used to make serial dilutions of OD_{600} 1, 0.1, 0.01, and 0.001 and 5 μl of each dilution was spotted on a SD-Leu-Trp plate as a growth control, and on a SD-Leu-Trp-Ade-His plate containing X-α-gal and supplemented with 0.2 μg/ml Aureobasidin A (Takara Bio, USA). Plates were imaged after incubation for 60–72 hr at 30˚C. Each experiment was repeated a minimum of three times, with similar results.

To assay the accumulation of protein in yeast cells, total yeast extracts were produced by harvesting cells from the liquid media and incubate them for 10 minutes at 95˚C after resuspending them in LDS Runblue sample buffer. Samples were then centrifugated and the supernatant was subjected to SDS-PAGE and western blot. The membranes were probed with anti-GAL4 DNA Binding domain (Sigma) antibody for the OsExo70F3 protein in pGBKT7 and with the anti-GAL4 activation domain (Sigma) antibody for AVR-Pii and ZiF effectors in pGADT7.

Protein-protein interaction: In planta co-immunoprecipitation (co-IP)

Transient gene expression was conducted by infiltrating 4-week-old *N*. *benthamiana* plants with *A*. *tumefaciens* strain GV3101 carrying 3xFLAG-OsExo70F2, 3xFLAG-mCherry, GFP-AVR-Pii, or GFP-AVR-Pii^{CCH}. Infiltrations were performed in ARM buffer (Agrobacterium resuspension medium, 10 mM MgCl2, 10 mM 2-(N-morpholine)-ethanesulfonic acid [MES], and pH 5.6) supplemented with 150 μM acetosyringone. Two leaves per *N*. *benthamiana* plant were infiltrated. After 72 hours samples were collected and frozen in liquid nitrogen. Protein extraction was carried out from 450 mg tissue samples, suspended in 2 mL IP buffer (25 mM Tris pH 7.5, 150 mM NaCl, 1 mM EDTA, 10% v/v glycerol, 2% w/v PVPP, 10 mM DTT, 1 cOmplete, EDTA free protease inhibitor tablet per 50 mL [Roche], and 0.1% Tween 20). After centrifugation at 4000 g for 30 minutes at 4˚C to clear the extracts, protein pull-downs were done by adding 30 μL of anti-FLAG magnetic beads (M2 anti-FLAG magnetic beads, Sigma). Samples were incubated in a rotary mixer for 2 h at 4˚C, washed 5 times with 1 ml IP buffer (25 mM Tris pH 7.5, 150 mM NaCl, 1 mM EDTA, 10% glycerol, and 0.1% Tween 20) and proteins eluted by adding 30 μL of 2x LDS sample buffer and incubating at 70˚C for 10 mins. 15–20 μL of the extracts were loaded on SDS–PAGE followed by immunoblot using either anti-FLAG (Cohesion Biosciences) or anti-GFP (Santa Cruz Biotechnology). Experiments were repeated at least two times.

Bioinformatic analyses: HMM search in fungal genomes

To develop a motif profile for the ZiF fold present in AVR-Pii, we first searched a database of candidate *M*. *oryzae* effectors [65] for sequences closely related to AVR-Pii using BLASTP from BLAST+ suite [66]. We extracted the sequences showing a match to AVR-Pii sequence with an E-value less than or equal to 0.0001. Next, we analysed these sequences using MEME [67] to identify a motif covering the amino acids involved in the ZiF fold. We used this ZiF fold motif alignment from MEME as an input to hmmbuild program from HMMER software (HMMER3/f 3.1b1, http://hmmer.org, May 2013) for creating a hidden Markov model (HMM) that represents the ZiF fold. We did motif searches against the proteomes of *M*. *oryzae* reported by Chiapello et al. [52] and Yoshida et al. [48] using the ZiF fold HMM and hmmsearch program from HMMER. We filtered out redundant sequences (100% identity) and sequences that do not contain a signal peptide as predicted by SignalP 3.0 [68] to achieve a non-redundant set of candidate ZiF effectors.

Bioinformatic analyses: TBLASTN search in *Magnaporthe* genomes

We used a TBLASTN-based approach to identify ZiF-effector members in 107 assemblies [21] that represent *Magnaporthe* isolates collected from 13 host plant species. We used each putative ZiF effector identified by HMM as individual queries for TBLASTN (E-value $\leq 1 \times 10^{-10}$) and extracted all hits with >80% query coverage. We then deduplicated the hits to generate a non-redundant list of ZIF effector variants and manually curated the hits to exclude TBLAST errors (e.g., start codon not detected by BLAST search algorithm or early termination of the alignments) and identified pseudogenes, defined by presence of premature stop codons or sequence deletions/insertions leading to reading frame change. This led to the identification of 95 putative ZiF effectors. ZiF effectors were classified using Markov Cluster algorithm (MCL) [69] with inflation value 1.4 and TRIBE-MCL option [70]. Alignments for each ZiF tribe were generated using Clustal Omega [71]. To identify presence/absence polymorphisms of these ZiF effector tribes in the collection of *Magnaporthe* isolates, we performed additional rounds of TBLASTN using 10 ZiF tribes containing the 95 ZiF effectors with the E-value threshold $\leq 1 \times 10^{-10}$ against those 107 genome assemblies.

Bioinformatic analyses: Alphafold2 prediction and structural comparison

To predict the structure of ZIF effector candidates, we first removed the signal peptide sequence of the 95 ZIF effector candidate. The processed sequences were then batch submitted to a local installation of Alphafold2 [56] using the default parameters. We then extracted the file ranked_-model_0.pdb of each ZIF effector for structural comparison. Automated structural comparison by TM-align failed because ZIF effectors contain a large, unstructured region at their N-terminus. We thus selected representative members of each tribe and superimposed them using ChimeraX [72] for structural comparison. To avoid errors during superimposition, we removed the unstructured region and used only the structured part of the protein (as shown in Fig 2).

Bioinformatic analyses: RNA-Seq analysis

Nucleotide sequences of Guy11_If, Guy11_Ik, Guy11_IIIj, Guy11_IVc, Guy11_Vc, Guy11_-Vic, Guy11_VIIc, Guy11_Xp and Guy11_Xi were used to retrieve the expression value from the RNA-seq reads with Kallisto [25,73]. TPM (transcripts per million) values were used to evaluate the expression profile of each candidate gene.

M. oryzae protoplast generation and transformation

Protoplast generation and transformation of *M. oryzae* isolate Sasa2 was carried out as described in Saitoh et al. [74]. Briefly, protoplasts were generated by inoculating 200 ml of Yeast Growth media (5 g of yeast extract, 20 g of glucose in 1 L dH_2O) with $\sim$10 cm^2 of mycelia grown on PDA plates and shaking at 121 rpm at $\sim$24˚C for 3 days. Mycelia was harvested via filtration and added to 15 ml lysing enzyme solution (from *Trichoderma harzianum*; Sigma-Aldrich) in a 50 ml tube. The tube was shaken at 45 rpm at 30˚C for 4 hours. Resulting protoplast suspension was filtered through two layers of Miracloth and collected in a clean tube. An equal volume of 0.6 M STC was added to the filtrate and centrifuged at 2,500 rpm at room temperature for 10 minutes and the supernatant discarded. Protoplasts were gently resuspended in 5 ml of 1 M STC. Additional resuspension and centrifugation steps were repeated with 30 ml, 25 ml, and 5 ml 1M STC sequentially, with the supernatant discarded between each wash step. Protoplasts were adjusted to a final concentration of 1×10^8 cells/ml.

For transformation, 60% PEG solution was added at a volume of 4x the volume of the protoplast suspension. Plasmid DNA solution (4 μg of DNA in 0.2 ml of H_2O) was added to 400 μl of

protoplast suspension and incubated on ice for 30 minutes. Sequential additions of 60% PEG solution were made of 0.2 ml, 0.3 ml, 0.6 ml, and 1.2 ml with gentle mixing of the solution. The resulting solution was left at room temperature for 15 minutes then centrifuged at 2,500 rpm for 10 minutes and the supernatant discarded. The protoplasts were gently resuspended in 0.3 ml 1 M STC and the final suspension spread onto selective media containing sulfonylurea. Transformants were recovered for 2 days at ~24˚C and monoconidial isolations collected.

Successful transformants were genotyped with AVR-Pii primers BTJP41_AVRPii_t3_p1f 5′–GCCTCTTCCTGTTCGCCA – 3′ and BTJP41_AVRPii_t3_p1r 5′–GTGGGAAGGG CTGCGATT – 3′. No amplification was observed from the Sasa2 wild type.

Rice blast infection assay

To evaluate the response of rice carrying Pii to rice blast fungal strain Sasa2 transformed with ZiF effectors from wheat blast lineages, we performed leaf drop infection assays in detached leaves from rice line Hitomebore (Pii+) and control susceptible line Moukoto (Pii-). Leaves were obtained from three-week old plants and placed on 1% agarose on square petri dishes.

Magnaporthe spores were collected from 10 days old cultures of the corresponding strain and diluted to a final concentration of $1x10^5$ conidia mL^{-1} in 0.2% gelatine. Leaves were inoculated with 20 μL of the conidia suspension with two leaves per treatment and 3 biological replicates. Lesions were imaged at 5 days post infection.

For spray inoculation, $1x10^5$ conidia mL^{-1} in 0.2% gelatine were sprayed on leaves of 3-weeks old plants and incubated for 5 days.

Supporting information

S1 Data. TBLAST results. Text files with hits for ZiF effectors by TBLAST for each *M. oryzae* isolate.
(ZIP)

S2 Data. List of amino acid sequences of each ZiF effector including secretion peptide.
(TXT)

S3 Data. Allele distribution of ZiF effectors in each *M. oryzae* isolate.
(XLSX)

S4 Data. Amino acid sequences of the identified ZiF effector in each *M. oryzae* isolate.
(TXT)

S5 Data. Raw RNAseq values in TPM (transcripts per million) for each ZiF effector from blast strain Guy11 during 8 infection timepoints.
(XLSX)

S6 Data. Uncropped western blots presented in this paper.
(PDF)

S1 Fig. Accumulation of AVR-Pii^{CCH} is compromised in yeast cells. Yeast lysate was probed for the expression of AVR-Pii effectors using anti-HA antibodies for the effectors fused to the GAL4 activation domain (AD). Total protein extracts were coloured with Coomassie Blue Stain (CBS).
(TIFF)

S2 Fig. Accumulation of AVR-Pii^{CCH} is compromised in plant cells. (A) Western blot analysis of N-terminally SH-tagged AVR-Pii or AVR-Pii^{CCH} transiently expressed in *N. benthamiana*. Plant lysates were probed with anti-HA antibodies for the presence of effectors. Total

protein extracts were colored with Coomassie Blue Stain (CBS). **(B)** Western blot analysis of N-terminally 3xFLAG-tagged AVR-Pii or AVR-Pii^{CCH} transiently expressed in rice protoplasts. Lysates from rice protoplasts were probed with anti-FLAG antibodies for the presence of AVR-Pii effectors. Total protein extracts were colored with Coomassie Blue Stain (CBS).
(TIFF)

S3 Fig. Properties of ZiF effector tribes. (A) Alignment of ZiF effector tribes showing conservation of the Zinc-finger motif and differences in residues forming the Exo70 binding interface. Protein sequence alignment of ZiF effector proteins reported here separated by tribes generated with Clustal Omega [71]. Residues contributing to the formation of a Zinc-finger motif are highlighted in yellow and residues at the equivalent positions of AVR-Pii binding interface [43] are highlighted in green. **(B)** Scores from hmmsearch and BLASTP search using ZiF HMM and Avr-Pii, respectively, against ZiF effector tribes.
(TIFF)

S4 Fig. Guy11 ZiF effectors are differentially expressed during infection in rice CO39 cultivar. Heatmap for expression of ZiF effectors at different times after infection (hpi). Expression is represented in shades of red or blue according to the centered expression levels as indicated. Only effectors for which we found expression are represented. Magnaporthe isolate Guy11 does not harbour AVR-Pii (ZiF_VIII).
(TIFF)

S5 Fig. Alignment of rice and wheat blast alleles of AVR-Pii showing conservation of the metal-binding and Exo70-binding interface residues. Protein sequence alignment of ZiF effector proteins ZiF_VIIId (AVR-Pii) and ZiF_VIIIc with Clustal Omega [71]. Secondary structure features based on AVR-Pii structure [43] are shown above. Residues contributing to the formation of a Zinc-finger motif are highlighted in yellow whereas the residues at the equivalent positions of AVR-Pii binding interface [43] are highlighted in green.
(TIFF)

S6 Fig. Protein accumulation in Yeast-2-Hybrid assay analysed by Western blot. Yeast lysate was probed for the presence of OsExo70F3, AVR-Pii, ZiF_VIIIc and their respective mutants using anti-GAL4 binding domain (BD) and anti-GAL4 DNA activation domain (AD) antibodies. Total protein extracts were stained with Coomassie Blue Stain (CBS). OsExo70F3 accumulation is consistently lower in positive interactions with ZiF effectors as noticed here and elsewhere in this and previous studies [43].
(TIFF)

S7 Fig. Alignment of grass Exo70 proteins showing conservation at the residues forming OsExo70F3 binding interface with AVR-Pii. Protein sequence alignment for the orthologs of AVR-Pii host targets, OsExo70F2 and OsExo70F3, from different grass species annotated by Holden et al. [54] (Os: *Oryza sativa*; Bd: *Brachypodium distachyon*; Hv: *Hordeum vulgare*; Ta: *Triticum aestivum*; Ot: *Oropetium thomaeum*; Si: *Setaria italica*; Sb: *Sorghum bicolor*; Zm: *Zea mays*). Sequence alignment was generated with Clustal Omega [71]. Residues at the equivalent positions of the OsExo70F2 binding interface with AVR-Pii are highlighted in red. Secondary structure features based on OsExo70F2 structure [43] are shown above.
(TIFF)

S8 Fig. Replicates of the disease resistance assays of Sasa2 harbouring AVR-Pii or ZiF_-VIIIc. First **(A),** second **(B)** and third **(C)** replicate of the rice leaf blade spot inoculation assay presented in **Fig 4**. Transgenic *M. oryzae* Sasa2 harbouring AVR-Pii or ZiF_VIIIc were spotted into rice cultivars Moukoto (Pii-) and Hitomebore (Pii+). The cultivars Moukoto and

Hitomebore are denoted by M and H, respectively. Wild-type rice blast isolate Sasa2 and wheat blast Br32 and BTJP 4–1 are included as controls.
(TIFF)

S9 Fig. Replicates of the spray inoculation disease resistance assays of Sasa2 harbouring AVR-Pii or ZiF_VIIIc. Four replicates of the rice leaf blade spray inoculation assay presented in Fig 4. Conidia from transgenic isolates of *M. oryzae* Sasa2 harbouring AVR-Pii or ZiF_VIIIc were sprayed into rice cultivars Moukoto (Pii-) and Hitomebore (Pii+) at a concentration of $1X10^5$ conidia mL^{-1} in 0.2% gelatine. Images were taken at 5 days post-infection. Wild-type rice blast isolate Sasa2 and wheat blast Br32 and BTJP 4–1 are included as controls.
(TIFF)

S10 Fig. Protein accumulation in rice blast Yeast-2-Hybrid assay analysed by Western blot. Yeast lysate was probed for the presence of OsExo70F3 using anti-GAL4 binding domain (BD) and the accumulation of selected rice blast ZiF effectors was probed with anti-GAL4 DNA activation domain (AD) antibodies. Total protein extracts were stained with Coomassie Blue Stain (CBS). OsExo70F3 accumulation is consistently lower in positive interactions with ZiF effectors as noticed here and elsewhere in this and previous studies [43].
(TIFF)

S11 Fig. Protein accumulation in wheat blast Yeast-2-Hybrid assay analysed by Western blot. Yeast lysate was probed for the presence of OsExo70F3 using anti-GAL4 binding domain (BD) while the accumulation of selected ZiF effectors from wheat blast lineages was probed with anti-GAL4 DNA activation domain (AD) antibodies. For technical feasibility, positive and negative controls AVR-Pii and AVR-Pii Phe65Glu were not included in the western blot as their production in yeast cells was tested before [43] and elsewhere in this study. Total protein extracts were stained with Coomassie Blue Stain (CBS). OsExo70F3 accumulation is consistently lower in positive interactions with ZiF effectors as noticed here and elsewhere in this and previous studies [43]. Due to the number of samples loaded on the SDS-PAGE gel before blotting, the molecular mass markers used in this specific figure are based on those of **S10 Fig** (see **S6 Data** for all uncropped blots).
(TIFF)

Acknowledgments

We thank current and past members of the "BLASTOFF" team from the Banfield, Kamoun, Terauchi and Talbot laboratories for discussion. We also thank Phil Robinson (JIC Photography) for help taking leaf images.

Author Contributions

Conceptualization: Juan Carlos De la Concepcion, Mark J. Banfield.

Data curation: Juan Carlos De la Concepcion, Thorsten Langner, Xia Yan, Joe Win.

Formal analysis: Juan Carlos De la Concepcion, Thorsten Langner, Xia Yan, Joe Win.

Funding acquisition: Nicholas J. Talbot, Ryohei Terauchi, Sophien Kamoun, Mark J. Banfield.

Investigation: Juan Carlos De la Concepcion, Thorsten Langner, Koki Fujisaki, Xia Yan, Vincent Were, Anson Ho Ching Lam, Indira Saado, Helen J. Brabham, Joe Win, Kentaro Yoshida.

Methodology: Thorsten Langner, Xia Yan, Joe Win.

Project administration: Juan Carlos De la Concepcion.

Resources: Helen J. Brabham, Nicholas J. Talbot, Ryohei Terauchi, Sophien Kamoun, Mark J. Banfield.

Supervision: Juan Carlos De la Concepcion, Nicholas J. Talbot, Mark J. Banfield.

Validation: Juan Carlos De la Concepcion, Xia Yan.

Visualization: Juan Carlos De la Concepcion, Thorsten Langner, Koki Fujisaki, Xia Yan, Joe Win.

Writing – original draft: Juan Carlos De la Concepcion, Thorsten Langner, Koki Fujisaki, Indira Saado, Mark J. Banfield.

Writing – review & editing: Juan Carlos De la Concepcion, Thorsten Langner, Koki Fujisaki, Xia Yan, Vincent Were, Anson Ho Ching Lam, Indira Saado, Helen J. Brabham, Joe Win, Kentaro Yoshida, Nicholas J. Talbot, Ryohei Terauchi, Sophien Kamoun, Mark J. Banfield.

References

1. Sanchez-Vallet A, Fouche S, Fudal I, Hartmann FE, Soyer JL, Tellier A, et al. The Genome Biology of Effector Gene Evolution in Filamentous Plant Pathogens. Annu Rev Phytopathol. 2018; 56:21–40. https://doi.org/10.1146/annurev-phyto-080516-035303 PMID: 29768136
2. Franceschetti M, Maqbool A, Jiménez-Dalmaroni MJ, Pennington HG, Kamoun S, Banfield MJ. Effectors of Filamentous Plant Pathogens: Commonalities amid Diversity. Microbiol Mol Biol Rev. 2017; 81 (2). https://doi.org/10.1128/MMBR.00066-16 PMID: 28356329
3. Seong K, Krasileva KV. Prediction of effector protein structures from fungal phytopathogens enables evolutionary analyses. Nature Microbiology. 2023; 8(1):174–87. https://doi.org/10.1038/s41564-022-01287-6 PMID: 36604508
4. Derbyshire MC, Raffaele S. Surface frustration re-patterning underlies the structural landscape and evolvability of fungal orphan candidate effectors. Nature Communications. 2023; 14(1):5244. https://doi.org/10.1038/s41467-023-40949-9 PMID: 37640704
5. Lovelace AH, Dorhmi S, Hulin MT, Li Y, Mansfield JW, Ma W. Effector Identification in Plant Pathogens. Phytopathology®. 2023; 113(4):637–50. https://doi.org/10.1094/PHYTO-09-22-0337-KD PMID: 37126080
6. Varden FA, De la Concepcion JC, Maidment JH, Banfield MJ. Taking the stage: effectors in the spotlight. Curr Opin Plant Biol. 2017; 38:25–33. https://doi.org/10.1016/j.pbi.2017.04.013 PMID: 28460241
7. de Guillen K, Ortiz-Vallejo D, Gracy J, Fournier E, Kroj T, Padilla A. Structure Analysis Uncovers a Highly Diverse but Structurally Conserved Effector Family in Phytopathogenic Fungi. PLoS Pathog. 2015; 11(10):e1005228. https://doi.org/10.1371/journal.ppat.1005228 PMID: 26506000
8. Lazar N, Mesarich CH, Petit-Houdenot Y, Talbi N, Li de la Sierra-Gallay I, Zelie E, et al. A new family of structurally conserved fungal effectors displays epistatic interactions with plant resistance proteins. PLoS Pathog. 2022; 18(7):e1010664. https://doi.org/10.1371/journal.ppat.1010664 PMID: 35793393
9. Yu DS, Outram MA, Smith A, McCombe CL, Khambalkar PB, Rima SA, et al. The structural repertoire of Fusarium oxysporum f. sp. lycopersici effectors revealed by experimental and computational studies. eLife. 2024; 12:RP89280. https://doi.org/10.7554/eLife.89280 PMID: 38411527
10. Rocafort M, Bowen JK, Hassing B, Cox MP, McGreal B, de la Rosa S, et al. The Venturia inaequalis effector repertoire is dominated by expanded families with predicted structural similarity, but unrelated sequence, to avirulence proteins from other plant-pathogenic fungi. BMC Biology. 2022; 20(1):246. https://doi.org/10.1186/s12915-022-01442-9 PMID: 36329441
11. Teulet A, Quan C, Evangelisti E, Wanke A, Yang W, Schornack S. A pathogen effector FOLD diversified in symbiotic fungi. New Phytol. 2023; 239(3):1127–39 https://doi.org/10.1111/nph.18996 PMID: 37257494
12. Le Naour-Vernet M, Charriat F, Gracy J, Cros-Arteil S, Ravel S, Veillet F, et al. Adaptive evolution in virulence effectors of the rice blast fungus Pyricularia oryzae. PLoS Pathog. 2023; 19(9):e1011294. https://doi.org/10.1371/journal.ppat.1011294 PMID: 37695773
13. Cao Y, Kümmel F, Logemann E, Gebauer JM, Lawson AW, Yu D, et al. Structural polymorphisms within a common powdery mildew effector scaffold as a driver of coevolution with cereal immune

receptors. Proceedings of the National Academy of Sciences. 2023; 120(32):e2307604120. https://doi.org/10.1073/pnas.2307604120 PMID: 37523523

14. Wilson RA, Talbot NJ. Under pressure: investigating the biology of plant infection by Magnaporthe oryzae. Nat Rev Microbiol. 2009; 7(3):185–95. https://doi.org/10.1038/nrmicro2032 PMID: 19219052
15. Eseola AB, Ryder LS, Oses-Ruiz M, Findlay K, Yan X, Cruz-Mireles N, et al. Investigating the cell and developmental biology of plant infection by the rice blast fungus Magnaporthe oryzae. Fungal genetics and biology: FG & B. 2021; 154:103562. https://doi.org/10.1016/j.fgb.2021.103562 PMID: 33882359
16. Latorre SM, Were VM, Foster AJ, Langner T, Malmgren A, Harant A, et al. Genomic surveillance uncovers a pandemic clonal lineage of the wheat blast fungus. PLoS Biol. 2023; 21(4):e3002052. https://doi.org/10.1371/journal.pbio.3002052 PMID: 37040332
17. Thierry M, Charriat F, Milazzo J, Adreit H, Ravel S, Cros-Arteil S, et al. Maintenance of divergent lineages of the Rice Blast Fungus Pyricularia oryzae through niche separation, loss of sex and post-mating genetic incompatibilities. PLoS Pathog. 2022; 18(7):e1010687. https://doi.org/10.1371/journal.ppat.1010687 PMID: 35877779
18. Gladieux P, Ravel S, Rieux A, Cros-Arteil S, Adreit H, Milazzo J, et al. Coexistence of Multiple Endemic and Pandemic Lineages of the Rice Blast Pathogen. mBio. 2018; 9(2): https://doi.org/10.1128/mBio.01806-17 PMID: 29615506
19. Barragan AC, Latorre SM, Mock PG, Harant A, Win J, Malmgren A, et al. Wild grass isolates of Magnaporthe (Syn. Pyricularia) spp. from Germany can cause blast disease on cereal crops. bioRxiv. 2022: 2022.08.29.505667.
20. Inoue Y, Vy TTP, Yoshida K, Asano H, Mitsuoka C, Asuke S, et al. Evolution of the wheat blast fungus through functional losses in a host specificity determinant. Science. 2017; 357(6346):80–3. https://doi.org/10.1126/science.aam9654 PMID: 28684523
21. Bentham AR, Petit-Houdenot Y, Win J, Chuma I, Terauchi R, Banfield MJ, et al. A single amino acid polymorphism in a conserved effector of the multihost blast fungus pathogen expands host-target binding spectrum. PLoS Pathog. 2021; 17(11):e1009957. https://doi.org/10.1371/journal.ppat.1009957 PMID: 34758051
22. Zdrzałek R, Stone C, De la Concepcion JC, Banfield MJ, Bentham AR. Pathways to engineering plant intracellular NLR immune receptors. Current Opinion in Plant Biology. 2023; 74:102380. https://doi.org/10.1016/j.pbi.2023.102380 PMID: 37187111
23. Cadiou L, Brunisholz F, Cesari S, Kroj T. Molecular engineering of plant immune receptors for tailored crop disease resistance. Current Opinion in Plant Biology. 2023; 74:102381. https://doi.org/10.1016/j.pbi.2023.102381 PMID: 37192575
24. Dean RA, Talbot NJ, Ebbole DJ, Farman ML, Mitchell TK, Orbach MJ, et al. The genome sequence of the rice blast fungus Magnaporthe grisea. Nature. 2005; 434(7036):980–6. https://doi.org/10.1038/nature03449 PMID: 15846337
25. Yan X, Tang B, Ryder LS, MacLean D, Were VM, Eseola AB, et al. The transcriptional landscape of plant infection by the rice blast fungus Magnaporthe oryzae reveals distinct families of temporally co-regulated and structurally conserved effectors. The Plant Cell. 2023; 35(5):1360–85. https://doi.org/10.1093/plcell/koad036 PMID: 36808541
26. De la Concepcion JC, Franceschetti M, Maqbool A, Saitoh H, Terauchi R, Kamoun S, et al. Polymorphic residues in rice NLRs expand binding and response to effectors of the blast pathogen. Nat Plants. 2018; 4(8):576–85. https://doi.org/10.1038/s41477-018-0194-x PMID: 29988155
27. Ortiz D, de Guillen K, Cesari S, Chalvon V, Gracy J, Padilla A, et al. Recognition of the Magnaporthe oryzae Effector AVR-Pia by the Decoy Domain of the Rice NLR Immune Receptor RGA5. The Plant cell. 2017; 29(1):156–68. https://doi.org/10.1105/tpc.16.00435 PMID: 28087830
28. Zhang Z-M, Zhang X, Zhou Z-R, Hu H-Y, Liu M, Zhou B, et al. Solution structure of the Magnaporthe oryzae avirulence protein AvrPiz-t. Journal of Biomolecular NMR. 2013; 55(2):219–23. https://doi.org/10.1007/s10858-012-9695-5 PMID: 23334361
29. Maidment JHR, Franceschetti M, Maqbool A, Saitoh H, Jantasuriyarat C, Kamoun S, et al. Multiple variants of the fungal effector AVR-Pik bind the HMA domain of the rice protein OsHIPP19, providing a foundation to engineer plant defence. J Biol Chem. 2021:100371.
30. Oikawa K, Fujisaki K, Shimizu M, Takeda T, Nemoto K, Saitoh H, et al. The blast pathogen effector AVR-Pik binds and stabilizes rice heavy metal-associated (HMA) proteins to co-opt their function in immunity. bioRxiv. 2024: 2020.12.01.406389.
31. De la Concepcion JC, Maidment JHR, Longya A, Xiao G, Franceschetti M, Banfield MJ. The allelic rice immune receptor Pikh confers extended resistance to strains of the blast fungus through a single polymorphism in the effector binding interface. PLOS Pathogens. 2021; 17(3):e1009368. https://doi.org/10.1371/journal.ppat.1009368 PMID: 33647072

32. Guo L, Cesari S, de Guillen K, Chalvon V, Mammri L, Ma M, et al. Specific recognition of two MAX effectors by integrated HMA domains in plant immune receptors involves distinct binding surfaces. Proc Natl Acad Sci U S A. 2018; 115(45):11637–42. https://doi.org/10.1073/pnas.1810705115 PMID: 30355769

33. Maqbool A, Saitoh H, Franceschetti M, Stevenson CE, Uemura A, Kanzaki H, et al. Structural basis of pathogen recognition by an integrated HMA domain in a plant NLR immune receptor. Elife. 2015; 4.

34. Białas A, Langner T, Harant A, Contreras MP, Stevenson CEM, Lawson DM, et al. Two NLR immune receptors acquired high-affinity binding to a fungal effector through convergent evolution of their integrated domain. eLife. 2021; 10:e66961. https://doi.org/10.7554/eLife.66961 PMID: 34288868

35. De la Concepcion JC, Vega Benjumea J, Białas A, Terauchi R, Kamoun S, Banfield MJ. Functional diversification gave rise to allelic specialization in a rice NLR immune receptor pair. Elife. 2021; 10.

36. Cesari S, Xi Y, Declerck N, Chalvon V, Mammri L, Pugnière M, et al. New recognition specificity in a plant immune receptor by molecular engineering of its integrated domain. Nature Communications. 2022; 13(1):1524. https://doi.org/10.1038/s41467-022-29196-6 PMID: 35314704

37. De la Concepcion JC, Franceschetti M, MacLean D, Terauchi R, Kamoun S, Banfield MJ. Protein engineering expands the effector recognition profile of a rice NLR immune receptor. eLife. 2019; 8:e47713. https://doi.org/10.7554/eLife.47713 PMID: 31535976

38. Liu Y, Zhang X, Yuan G, Wang D, Zheng Y, Ma M, et al. A designer rice NLR immune receptor confers resistance to the rice blast fungus carrying noncorresponding avirulence effectors. Proc Natl Acad Sci U S A. 2021; 118(44).

39. Bentham AR, De la Concepcion JC, Benjumea JV, Kourelis J, Jones S, Mendel M, et al. Allelic compatibility in plant immune receptors facilitates engineering of new effector recognition specificities. The Plant Cell. 2023; 35(10):3809–27. https://doi.org/10.1093/plcell/koad204 PMID: 37486356

40. Maidment JHR, Shimizu M, Bentham AR, Vera S, Franceschetti M, Longya A, et al. Effector target-guided engineering of an integrated domain expands the disease resistance profile of a rice NLR immune receptor. eLife. 2023; 12:e81123. https://doi.org/10.7554/eLife.81123 PMID: 37199729

41. Kourelis J, Marchal C, Posbeyikian A, Harant A, Kamoun S. NLR immune receptor–nanobody fusions confer plant disease resistance. Science. 2023; 379(6635):934–9. https://doi.org/10.1126/science.abn4116 PMID: 36862785

42. Rodriguez-Moreno L, Song Y, Thomma BP. Transfer and engineering of immune receptors to improve recognition capacities in crops. Curr Opin Plant Biol. 2017; 38:42–9. https://doi.org/10.1016/j.pbi.2017.04.010 PMID: 28472757

43. De la Concepcion JC, Fujisaki K, Bentham AR, Cruz Mireles N, Sanchez de Medina Hernandez V, Shimizu M, et al. A blast fungus zinc-finger fold effector binds to a hydrophobic pocket in host Exo70 proteins to modulate immune recognition in rice. Proceedings of the National Academy of Sciences. 2022; 119(43):e2210559119. https://doi.org/10.1073/pnas.2210559119 PMID: 36252011

44. Fujisaki K, Abe Y, Ito A, Saitoh H, Yoshida K, Kanzaki H, et al. Rice Exo70 interacts with a fungal effector, AVR-Pii, and is required for AVR-Pii-triggered immunity. Plant J. 2015; 83(5):875–87. https://doi.org/10.1111/tpj.12934 PMID: 26186703

45. Fujisaki K, Abe Y, Kanzaki E, Ito K, Utsushi H, Saitoh H, et al. An unconventional NOI/RIN4 domain of a rice NLR protein binds host EXO70 protein to confer fungal immunity. bioRxiv. 2017:239400.

46. Yoshida K, Saitoh H, Fujisawa S, Kanzaki H, Matsumura H, Yoshida K, et al. Association genetics reveals three novel avirulence genes from the rice blast fungal pathogen Magnaporthe oryzae. The Plant cell. 2009; 21(5):1573–91. https://doi.org/10.1105/tpc.109.066324 PMID: 19454732

47. Białas A, Zess EK, De la Concepcion JC, Franceschetti M, Pennington HG, Yoshida K, et al. Lessons in Effector and NLR Biology of Plant-Microbe Systems. Mol Plant Microbe Interact. 2018; 31(1):34–45. https://doi.org/10.1094/MPMI-08-17-0196-FI PMID: 29144205

48. Yoshida K, Saunders DG, Mitsuoka C, Natsume S, Kosugi S, Saitoh H, et al. Host specialization of the blast fungus Magnaporthe oryzae is associated with dynamic gain and loss of genes linked to transposable elements. BMC Genomics. 2016; 17:370. https://doi.org/10.1186/s12864-016-2690-6 PMID: 27194050

49. Latorre SM, Reyes-Avila CS, Malmgren A, Win J, Kamoun S, Burbano HA. Differential loss of effector genes in three recently expanded pandemic clonal lineages of the rice blast fungus. BMC Biol. 2020; 18(1):88. https://doi.org/10.1186/s12915-020-00818-z PMID: 32677941

50. Seong K, Krasileva KV. Computational Structural Genomics Unravels Common Folds and Novel Families in the Secretome of Fungal Phytopathogen Magnaporthe oryzae. Mol Plant Microbe Interact. 2021; 34(11):1267–80. https://doi.org/10.1094/MPMI-03-21-0071-R PMID: 34415195

51. Win J, Krasileva KV, Kamoun S, Shirasu K, Staskawicz BJ, Banfield MJ. Sequence divergent RXLR effectors share a structural fold conserved across plant pathogenic oomycete species. PLoS Pathog. 2012; 8(1):e1002400. https://doi.org/10.1371/journal.ppat.1002400 PMID: 22253591

52. Chiapello H, Mallet L, Guérin C, Aguileta G, Amselem J, Kroj T, et al. Deciphering Genome Content and Evolutionary Relationships of Isolates from the Fungus Magnaporthe oryzae Attacking Different Host Plants. Genome Biology and Evolution. 2015; 7(10):2896–912. https://doi.org/10.1093/gbe/evv187 PMID: 26454013

53. Mosquera G, Giraldo MC, Khang CH, Coughlan S, Valent B. Interaction Transcriptome Analysis Identifies Magnaporthe oryzae BAS1-4 as Biotrophy-Associated Secreted Proteins in Rice Blast Disease The Plant Cell. 2009; 21(4):1273–90.

54. Holden S, Bergum M, Green P, Bettgenhaeuser J, Hernández-Pinzón I, Thind A, et al. A lineage-specific Exo70 is required for receptor kinase–mediated immunity in barley. Science Advances. 2022; 8 (27):eabn7258. https://doi.org/10.1126/sciadv.abn7258 PMID: 35857460

55. Sperschneider J. Machine learning in plant–pathogen interactions: empowering biological predictions from field scale to genome scale. New Phytologist. 2020; 228(1):35–41. https://doi.org/10.1111/nph.15771 PMID: 30834534

56. Jumper J, Evans R, Pritzel A, Green T, Figurnov M, Ronneberger O, et al. Highly accurate protein structure prediction with AlphaFold. Nature. 2021; 596(7873):583–9. https://doi.org/10.1038/s41586-021-03819-2 PMID: 34265844

57. Homma F, Huang J, van der Hoorn RAL. AlphaFold-Multimer predicts cross-kingdom interactions at the plant-pathogen interface. Nature Communications. 2023; 14(1):6040. https://doi.org/10.1038/s41467-023-41721-9 PMID: 37758696

58. Mukhi N, Gorenkin D, Banfield MJ. Exploring folds, evolution and host interactions: understanding effector structure/function in disease and immunity. New Phytologist. 2020; 227(2):326–33. https://doi.org/10.1111/nph.16563 PMID: 32239533

59. Bailey PC, Schudoma C, Jackson W, Baggs E, Dagdas G, Haerty W, et al. Dominant integration locus drives continuous diversification of plant immune receptors with exogenous domain fusions. Genome Biol. 2018; 19(1):23. https://doi.org/10.1186/s13059-018-1392-6 PMID: 29458393

60. Brabham HJ, Hernández-Pinzón I, Holden S, Lorang J, Moscou MJ. An ancient integration in a plant NLR is maintained as a trans-species polymorphism. bioRxiv. 2018:239541.

61. Kim S, Kim C-Y, Park S-Y, Kim K-T, Jeon J, Chung H, et al. Two nuclear effectors of the rice blast fungus modulate host immunity via transcriptional reprogramming. Nature Communications. 2020; 11 (1):5845. https://doi.org/10.1038/s41467-020-19624-w PMID: 33203871

62. Kanzaki H, Yoshida K, Saitoh H, Fujisaki K, Hirabuchi A, Alaux L, et al. Arms race co-evolution of Magnaporthe oryzae AVR-Pik and rice Pik genes driven by their physical interactions. Plant J. 2012; 72 (6):894–907. https://doi.org/10.1111/j.1365-313X.2012.05110.x PMID: 22805093

63. Ichimaru K, Yamaguchi K, Harada K, Nishio Y, Hori M, Ishikawa K, et al. Cooperative regulation of PBI1 and MAPKs controls WRKY45 transcription factor in rice immunity. Nature Communications. 2022; 13(1):2397. https://doi.org/10.1038/s41467-022-30131-y PMID: 35577789

64. Ishikawa K, Yamaguchi K, Sakamoto K, Yoshimura S, Inoue K, Tsuge S, et al. Bacterial effector modulation of host E3 ligase activity suppresses PAMP-triggered immunity in rice. Nature Communications. 2014; 5(1):5430. https://doi.org/10.1038/ncomms6430 PMID: 25388636

65. Petit-Houdenot Y, Langner T, Harant A, Win J, Kamoun S. A Clone Resource of Magnaporthe oryzae Effectors That Share Sequence and Structural Similarities Across Host-Specific Lineages. Mol Plant Microbe Interact. 2020; 33(8):1032–5. https://doi.org/10.1094/MPMI-03-20-0052-A PMID: 32460610

66. Camacho C, Coulouris G, Avagyan V, Ma N, Papadopoulos J, Bealer K, et al. BLAST+: architecture and applications. BMC Bioinformatics. 2009; 10(1):421. https://doi.org/10.1186/1471-2105-10-421 PMID: 20003500

67. Bailey TL, Johnson J, Grant CE, Noble WS. The MEME Suite. Nucleic Acids Res. 2015; 43(W1):W39–49. https://doi.org/10.1093/nar/gkv416 PMID: 25953851

68. Bendtsen JD, Nielsen H, von Heijne G, Brunak S. Improved prediction of signal peptides: SignalP 3.0. J Mol Biol. 2004; 340(4):783–95. https://doi.org/10.1016/j.jmb.2004.05.028 PMID: 15223320

69. Dongen SV. Graph Clustering Via a Discrete Uncoupling Process. SIAM Journal on Matrix Analysis and Applications. 2008; 30(1):121–41.

70. Enright AJ, Van Dongen S, Ouzounis CA. An efficient algorithm for large-scale detection of protein families. Nucleic Acids Res. 2002; 30(7):1575–84. https://doi.org/10.1093/nar/30.7.1575 PMID: 11917018

71. Sievers F, Higgins DG. Clustal Omega, accurate alignment of very large numbers of sequences. Methods Mol Biol. 2014; 1079:105–16. https://doi.org/10.1007/978-1-62703-646-7_6 PMID: 24170397

72. Pettersen EF, Goddard TD, Huang CC, Meng EC, Couch GS, Croll TI, et al. UCSF ChimeraX: Structure visualization for researchers, educators, and developers. Protein Sci. 2021; 30(1):70–82. https://doi.org/10.1002/pro.3943 PMID: 32881101

73. Bray NL, Pimentel H, Melsted P, Pachter L. Near-optimal probabilistic RNA-seq quantification. Nature Biotechnology. 2016; 34(5):525–7. https://doi.org/10.1038/nbt.3519 PMID: 27043002

74. Saitoh H, Fujisawa S, Mitsuoka C, Ito A, Hirabuchi A, Ikeda K, et al. Large-Scale Gene Disruption in Magnaporthe oryzae Identifies MC69, a Secreted Protein Required for Infection by Monocot and Dicot Fungal Pathogens. PLOS Pathogens. 2012; 8(5):e1002711. https://doi.org/10.1371/journal.ppat.1002711 PMID: 22589729